

**Extended dust emission and atomic hydrogen,
a reservoir of diffuse H₂ in NGC 1068**

Padeli. P. Papadopoulos

Sterrewacht Leiden, P. O. Box 9513, 2300 RA Leiden, The Netherlands

and

E. R. Seaquist

Department of Astronomy, University of Toronto, 60 St. George st. Toronto,
ON M5S-3H8, Canada.

Received _____; accepted _____

ABSTRACT

We report on sensitive sub-mm imaging observations of the prototype Seyfert 2/starburst galaxy NGC 1068 at 850 μm and 450 μm using the Submillimetre Common-User Bolometer Array (SCUBA) on the James Clerk Maxwell Telescope (JCMT). We find clear evidence of dust emission associated with the extended HI component which together with the very faint ^{12}CO J=1–0 emission give a gas-to-dust ratio of $M_{\text{gas}}/M_{\text{dust}} \sim 70 - 150$. This contrasts with the larger ratio $M_{\text{gas}}/M_{\text{dust}} \sim 330$ estimated within a galactocentric radius of $r \leq 1.36$ kpc, where the gas is mostly molecular and starburst activity occurs. The large gas-to-dust ratio found for the starburst region is attributed to a systematic overestimate of the molecular gas mass in starburst environments when the luminosity of the ^{12}CO J=1–0 line and a standard galactic conversion factor is used. On the other hand sub-mm imaging proves to be a more powerful tool than conventional CO imaging for revealing the properties of the diffuse H_2 that coexists with HI. This molecular gas phase is characterized by low densities ($n(\text{H}_2) < 10^3 \text{ cm}^{-3}$), very faint emission from sub-thermally excited CO, and contains more mass than HI, namely $M(\text{H}_2)/M(\text{HI}) \sim 5$.

Subject headings: ISM: dust, molecules and atoms — galaxies: individual (NGC 1068)

1. Introduction

The standard way to estimate molecular gas mass in galaxies uses the luminosity of the ^{12}CO J=1–0 line and converts it to molecular gas mass by using the so-called standard galactic conversion factor X_{co} (e.g. Young & Scoville 1982; Bloemen 1985; Dickman et al. 1986; Young & Scoville 1991). The dependence of X_{co} on the ambient conditions of the molecular gas has been extensively explored. The main factors are: a) metallicity and the intensity of the ambient UV radiation field (e.g. Israel 1988; Wilson 1995; Arimoto, Sofue & Tsujimoto 1996; Israel 1997), b) the density, temperature, and kinematic state of the average molecular cloud and, c) effects of particular geometries (e.g. see Bryant & Scoville 1996; Sakamoto 1996 for a recent exposition). In the environments of extreme starbursts it has been clearly demonstrated that the standard method overestimates $M(\text{H}_2)$ since it yields masses comparable or larger than the dynamical ones (e.g. Downes, Solomon & Radford 1993; Bryant & Scoville 1996; Solomon et al. 1997; Downes & Solomon 1998). In low metallicity environments with high UV intensities the larger rate of CO dissociation with respect to H_2 produces a lower CO luminosity per H_2 and thus underestimates $M(\text{H}_2)$.

In principle the aforementioned effects can be taken into account by a combination of observational and theoretical work studying a wide range of galactic environments, which can then provide “adjusted” X_{co} factors to be used for the appropriate set of conditions. However little can be done if the H_2 is so diffuse and/or cold that the ^{12}CO J=1–0 line is very faint or not luminous at all. Hints of such physical conditions have been recently reported for the outer parts of Milky Way (Usuda et al. 1998) and cold dense clouds have been reported for M 31 (Loinard & Allen 1998). In such cases the advantage of easily detecting and mapping a bright CO line and thus the distribution of H_2 is lost. Here we report deep sub-mm imaging of the prototype Sy2/starburst galaxy NGC 1068 that reveals extended emission from dust well beyond the CO-bright regions and associated with the HI.

2. Observations

The observations were made on two nights in 1997 August 4 and 1998 January 26 with the Sub-mm Common User Bolometer Array (SCUBA) at the 15 m James Clerk Maxwell Telescope (JCMT)¹. SCUBA is a dual camera system cooled well below 1 K that allows sky-background limited simultaneous observations with two arrays. The short-wavelength array contains 91 pixels and the long-wavelength array 37 pixels. Both arrays have approximately the same field of view on the sky $\sim 2.3'$. For a full description of the instrument see Holland et al. 1998.

We performed dual wavelength imaging at 450 μm and 850 μm using the 64-point jiggle mapping mode that allows Nyquist sampling of the field of view (Holland et al. 1998). We employed the recommended rapid beam switching at a frequency of 8 Hz and a beam throw of 120'' in azimuth. The pointing and focus of the telescope were monitored frequently using Mars, Jupiter and CRL 618, with an expected rms pointing error of $\leq 3''$. All the NGC 1068 maps were bracketed by skydips used to correct for atmospheric extinction. Typical opacities at 850 μm were $\tau \sim 0.14$ for our 1998 run and $\tau \sim 0.6$ for our 1997 run. Frequent photometric measurements and beam maps of CRL 618 and Mars allowed close monitoring of the gains (Jy/beam Volt⁻¹). These can vary significantly especially at 450 μm if the dish has not thermally relaxed and can even be elevation dependent (Sandell 1998).

The individual jiggle maps are consistent in terms of peak and integrated intensities and were co-added after flatfielding, correcting for atmospheric extinction, and editing out bad bolometers/integrations using the standard reduction package SURF

¹The JCMT is operated by the Joint Astronomy Center in Hilo, Hawaii on behalf of the parent organizations PPARC in the United Kingdom, the National Research Council of Canada and the The Netherlands Organization for Scientific Research.

(Jenness & Lightfoot 1998). Special care was taken to remove sky-noise using bolometers at the edge of the field of view that “look” at sky emission only (Jenness, Lightfoot & Holland 1998). As a result the final maps have exceptional sensitivity, close to the one expected from the total integration time and the NEFDs at the sky conditions of our runs. Flux calibration of the final maps in mJy/beam was obtained from beam maps of CRL 618 obtained with the same chop throw as our NGC 1068 maps. The corresponding beam profiles were obtained from beam maps of CRL 618 and Mars. The calibration information is summarized in Table 1.

EDITOR: PLACE TABLE 1 HERE

3. Extended sub-mm emission: CO, HI and dust

The clear association of the sub-mm emission from dust and HI gas is demonstrated in Figure 1 where the 850 μm and 450 μm maps are overlaid with an HI map (Brinks et al. 1994) at a common resolution of $\sim 15''$. Figure 2 shows the bright central 450 μm emission and the associated ^{12}CO J=1–0 integrated brightness (Helfer & Blitz 1995) that lie within the central HI “hole” seen in Figure 1. This wealth of imaging data for the ISM in NGC 1068 and the wide range of conditions present due to the existence of the central starburst (Telesco et al. 1984) make it an ideal testing “ground” of our standard ideas about the distribution and mass of the various ISM phases on large scales. We adopt a distance to NGC 1068 of 14 Mpc ($H_0 = 75 \text{ km s}^{-1} \text{ Mpc}^{-1}$) where $1'' = 68 \text{ pc}$.

A remarkable property of the sub-mm emission is that it extends over the entire bright HI emission where the estimated $R = S_{450}/S_{850}$ ratio is lower than in the CO-bright region where the starburst occurs. This ratio and its variations across the image can be a

good temperature indicator as long as the average dust temperature is $T \leq 30$ K. Indeed, assuming a single average dust component, this ratio can be expressed as

$$\frac{S_{450}}{S_{850}} = 1.88^{\beta+3} \left(\frac{e^{16.8/T} - 1}{e^{31.8/T} - 1} \right), \quad (1)$$

where β is the emissivity law. It can be easily seen that the ratio tends to the R-J limit for dust temperatures of $T \geq 30$ K and is no longer temperature-sensitive. Nevertheless, for a range of $T = 10 - 30$ K, it varies by a factor of ~ 2 . This temperature range is particularly interesting since it “marks” the transition between cool and warm dust, the latter dominating the IRAS 100 μ m and 60 μ m bands.

After carefully correcting the integrated flux densities for the error beam contribution (Sandell 1998) using the correction factors tabulated in Table 1, we obtain $R(r \leq 20'') = 7.10 \pm 1.77$. For $\beta = 2$ this agrees well with the range of gas temperatures $T \sim 20 - 30$ K found from studying the CO excitation within this region (Papadopoulos & Seaquist 1998) and the minimum temperature of ~ 20 K implied from the observed ^{12}CO J=1–0 brightness temperatures in high resolution maps (e.g. Planesas, Scoville, & Myers 1991). For the sub-mm emission associated with the HI distribution we find $R(20'' \leq r \leq 60'') = 4.70 \pm 1.17$. This ratio suggests colder gas, in the range of $T \sim 10 - 15$ K, but rules out any M 31-type clouds (Loinard & Allen 1998) where $T_{\text{kin}} < 10$ K. Here we must emphasize that the main uncertainty in the estimate of R is due to systematic factors ($\sim 25\%$) that stay unchanged across the maps. The thermal rms uncertainty is $\leq 5\%$ and thus the observed change of R between the CO-bright and the HI-bright regions is much more significant than the total quoted uncertainties imply.

4. The gas-to-dust ratio

The spatial resolution of our sub-mm maps and the HI, ^{12}CO J=1–0 maps from the literature permits us to estimate the gas/dust ratio as a function of position in this galaxy. Combining the standard expressions for the HI, H_2 and dust mass the gas/dust ratio in astrophysical units is expressed as follows:

$$\frac{M_g}{M_d} \approx 1.25 \times 10^3 \left(\frac{\nu}{\nu_o} \right)^{\beta+3} \left(e^{h\nu/kT} - 1 \right)^{-1} \left[\frac{S_{\text{HI}} + 10^{-2} X_{\text{co}} S_{\text{CO}}}{S_\nu} \right], \quad (2)$$

where S_{HI} and S_{CO} are the velocity-integrated flux densities of the HI hyperfine transition and the ^{12}CO J=1–0 line respectively in Jy km s^{-1} , X_{co} is the standard galactic conversion factor in units of $M_\odot (\text{K km s}^{-1} \text{ pc}^2)^{-1}$ and S_ν is the sub-mm flux density at frequency ν in Jy. We adopted the emissivity law given by Hildebrand (1983), namely $k(\nu) = k(\nu_o) (\nu/\nu_o)^\beta$, where $k(\nu_o) = 10 \text{ cm}^{-2} \text{ gr}$ and $\nu_o = 1196 \text{ GHz}$ ($250 \mu\text{m}$).

For a galactocentric radius of $r = 20''$, where most of the FIR emission arises (Telesco et al. 1984), we estimate $S_{\text{CO}} = (2800 \pm 800) \text{ Jy km s}^{-1}$ (from the ^{12}CO J=1–0 channel maps, Helfer & Blitz 1995), $S_{\text{HI}} = (0.82 \pm 0.20) \text{ Jy km s}^{-1}$ and $S_{450} = (8.74 \pm 1.95) \text{ Jy}$, $S_{850} = (1.23 \pm 0.13) \text{ Jy}$. For $\beta = 2$ and $X_{\text{co}} = 5 M_\odot (\text{K km s}^{-1} \text{ pc}^2)^{-1}$ (i.e. the standard galactic value), the observed $850 \mu\text{m}$ flux density implies

$$\frac{M_g}{M_d} \approx 315 \left(e^{16.8/T} - 1 \right)^{-1}, \quad (3)$$

For $T = 25 \text{ K}$ yields $M_g/M_d \sim 330$, similar to the molecular gas-to-dust ratio found in spirals using IRAS $100 \mu\text{m}$ and $60 \mu\text{m}$ fluxes (Young et al. 1986; Young et al. 1989).

Assuming that the actual gas-to-dust ratio in NGC 1068 is similar to that for the Milky Way, namely 100-150, we conclude that the application of equation (3) leads to a significant

overestimate of this ratio for the inner region ($r \leq 20''$) of NGC 1068. There is indeed independent evidence (e.g. Downes & Solomon 1998) which suggests that the standard galactic conversion factor applied to starburst nuclei leads to significant overestimates the H_2 content in these regions. In addition, Papadopoulos & Seaquist (1998) provide indications that $M(H_2)$ in the inner region of NGC 1068 is overestimated by a factor of two, which would then produce agreement between the ratio for the nuclear region NGC 1068 and the Milky way.

For $r > 20''$, no bright CO emission is detected (see Fig. 2, Helfer & Blitz 1995). There is, however, evidence for faint CO emission. By integrating over the area $20'' \leq r \leq 60''$ we find $S_{CO} = (1570 \pm 470)$ Jy km s⁻¹. Over the same area, we estimate $S(HI) = (16 \pm 1)$ Jy km s⁻¹ and $S_{450} = (4.0 \pm 0.9)$ Jy, $S_{850} = (0.85 \pm 0.09)$ Jy. Using these figures, together with equation (2) and the standard value for X_{co} , we obtain,

$$\frac{M_g}{M_d} \approx 300 \left(e^{16.8/T} - 1 \right)^{-1}, \quad (4)$$

For $T \sim 10 - 15$ K we obtain $M_g/M_d = 70 - 150$ and $M(H_2)/M(HI) \sim 5$. The good agreement of the gas-to-dust ratio with that of the Milky way suggests that most of the gas/dust mass is accounted for.

However, the CO becomes exceedingly faint and essentially undetectable at $r \geq 30''$. If we assume the lowest gas/dust temperature of $T \sim 10$ K allowed by the S_{450}/S_{850} ratio, the inferred gas-to-dust ratio for $30'' \leq r \leq 60''$ would be ~ 40 with $M(H_2)/M(HI) \sim 1$ (using the standard X_{co}). Thus, the use of the standard conversion factor in this region may underestimate $M(H_2)$ by a factor of ~ 5 . It seems possible that this molecular gas phase is not CO-bright mainly because of low densities ($n(H_2) < 10^3$ cm⁻³) rather than low gas/dust temperatures. A thermalized ¹²CO J=1–0 line would remain luminous as long as $T \geq \Delta E_{10}/k \sim 5$ K, and lower temperatures would yield $S_{450}/S_{850} \leq 1.13$ which is not

observed. Assuming similar spatial and velocity filling factors, we estimate that the average ^{12}CO J=1–0 brightness temperature for the outer regions $T_b \sim 0.07 \times T_b(r \leq 20'')$. For the various molecular clouds (size ~ 200 pc) within the $r \sim 20''$ radius $T_b(r \leq 20'') \sim 10 - 20$ K (e.g. Planesas, Scoville & Myers 1991), hence for similar size molecular clouds in the HI-bright regions it would be $T_b \sim 1$ K. This is significantly lower than the gas/dust temperature inferred by the S_{450}/S_{850} ratio over the same regions, thus implying sub-thermally excited ^{12}CO J=1–0.

These characteristics of the diffuse H_2 phase makes sub-mm measurements very valuable since, while CO is very faint and may underestimate the H_2 mass, the dust/gas temperature is still high enough to allow sub-mm imaging to reveal the distribution and mass of the H_2 mixed with HI, under the assumption of a canonical gas-to-dust ratio. We expect this gas phase to be a general feature in spiral galaxies and sensitive sub-mm imaging of the regions with high HI column densities is a new tool to study its properties through the associated dust emission.

5. Conclusions

The results of deep sub-mm imaging of the archetypal Seyfert 2/starburst galaxy NGC 1068 can be summarized as follows:

1. Extended sub-mm emission due to dust with a temperature of $T \sim 10 - 15$ K is found associated with the regions with the highest HI column densities. A more spatially concentrated and warmer ($T \sim 20 - 30$ K) component is found in the inner starburst region where most of the gas is molecular. The estimated gas-to-dust ratio for the inner region is $M_g/M_d \sim 330$ while for the dust emission associated with the HI gas we find $M_g/M_d \sim 70 - 150$ depending on the value of the gas/dust temperature.

2. Under the assumption that a Milky Way value of $M_g/M_d \sim 100 - 150$ applies also to NGC 1068, we conclude that the high value of M_g/M_d in its starburst region is a result of an overestimate of the molecular gas mass. This seems to be a systematic effect of using the standard galactic conversion factor to convert $^{12}\text{CO J=1-0}$ luminosity to molecular gas mass in starburst environments.

3. The diffuse H_2 gas that is mixed with the HI gas is associated with sub-thermally excited and very faint CO emission. Furthermore it is more massive than HI, with $M(\text{H}_2)/M(\text{HI}) \sim 5$ and the standard galactic conversion factor may underestimate $M(\text{H}_2)$ at low gas/dust temperatures of $T \sim 10$ K. For this gas phase sensitive sub-mm imaging provides a better tool than CO imaging in revealing its distribution and mass.

We thank Rob Ivison and Lorne Avery for conducting a wonderful set of observations with SCUBA, and Wayne Holland for friendly and useful advice. We are grateful to Elias Brinks for the HI map and Tamara Helfer for the $^{12}\text{CO J=1-0}$ map. E. R. S acknowledges the support of a research grant from the Natural Sciences and Engineering Research Council of Canada.

REFERENCES

- Loinard, L., & Allen, R. J. 1998, ApJ, 499, 227
- Arimoto, N., Sofue, Y., & Tsujimoto, T. 1996, Publ. of the Astronomical Society of Japan, v.48, p. 275-284
- Bloemen, J. B. G. M. 1985, PhD thesis, University of Leiden
- Brinks, E., Skillman, E. D., Terlevich, R. J. & Terlevich, E. 1994, in Proceedings of the 159th Symposium of the IAU 1994, vol 159, p. 422
- Bryant, P. M., & Scoville, N. Z. 1996, ApJ, 457, 678
- Dickman, R. L., Snell, R. L., & Schloerb, F. P. 1986, ApJ, 309, 326
- Downes, D., Solomon, P. M., & Radford, S. J. E. 1993, ApJ, 414, 13
- Downes, D., & Solomon, P. M. 1998, ApJ, 507, 615
- Helfer, T. T., & Blitz, L. 1995, ApJ, 450, 90
- Hildebrand, R. H. 1983, MNRAS, 24, 267
- Holland, W. S., Robson, E. I., Gear, W. K., Cunningham, C. R., Lightfoot, J. F., Jenness, T., Ivison, R. J., Stevens, J. A., Ade, P. A. R., Griffin, M. J., Duncan W. D., Murphy J. A., & Naylor, D. A. 1998 MNRAS(in press), astro-ph/9809122
- Israel, F. P. 1988, in *Millimetre and Submillimetre Astronomy*, pg 281, (Eds R. D. Wolstencroft and W. B. Burton) Kluwer Academic Publishers
- Israel, F. P. 1997, A&A, 328, 471
- Jenness, T., & Lightfoot, J. F. 1998 in SURF-SCUBA User Reduction Facility, User's manual

- Jenness, T., Lightfoot, J. F., & Holland, W. S. 1998, astro-ph/9809120
- Papadopoulos, P. P., & Seaquist, E. R. 1998, ApJ, in press
- Planesas, P., Scoville, N. Z., & Myers, S. T. 1991, ApJ, 369, 364
- Sakamoto, S. 1996, ApJ, 462, 215
- Sandell, G. 1998, The SCUBA mapping cookbook A first step to proper map reduction.
- Solomon, P. M., Downes, D., Radford, S. J. E., & Barrett, J. W. 1997, ApJ, 478, 144
- Telesco, C. M., Becklin, E. E., Wynn-Williams, C. G., & Harper, D. A. 1984, ApJ, 282, 427
- Usuda, K. S., Hasegawa, T., Handa, T., Morino, J.-I., Sawada, T., Sakamoto, S., Oka, T., Seta, M., Hayashi, M., Booth, R., Nyman, L.-A., Bronfman, L., May, J., Castellanos, A. L., Shaver, P., White, G. J. in *The Physics and Chemistry of the Interstellar Medium*, Abstract Book of the 3rd Cologne-Zermatt Symposium, held in Zermatt, September 22-25, 1998, Ed.: V. Ossenkopf Shaker-Verlag Aachen.
- Wilson, C. D. 1995, ApJ, 448, 97
- Young, J. S., & Scoville, N. Z. 1982, ApJ, 258, 467
- Young, J. S., Schloerb, F. P., Kenney, J. D., & Lord, S. D. 1986, ApJ, 304, 443
- Young, J. S., Xie, S., Kenney, J. D., & Rice, W. L. 1989, ApJS, 70, 699
- Young, J. S., & Scoville, N. Z. 1991, ARA&A, 29, 581

Fig. 1.— Grey scale: Velocity-integrated HI brightness with a range of $100 - 830$ mJy beam $^{-1}$ km s $^{-1}$, and $\sigma_{\text{rms}} \sim 100$ mJy beam $^{-1}$ km s $^{-1}$.

Contours: 850 μm brightness (top), 450 μm brightness (bottom). The contours are: (1, 2, 3, 4, 5, 7, 10, 15, 20, 25, 30, 35) $\times\sigma$, where $\sigma_{\text{rms}}(850 \mu\text{m}) = 10$ mJy beam $^{-1}$ and $\sigma_{\text{rms}}(450 \mu\text{m}) = 90$ mJy beam $^{-1}$. The resolution of all the maps is $\sim 15''$.

Fig. 2.— Gray scale: Velocity-integrated ^{12}CO J=1–0 brightness from Helfer & Blitz 1995, convolved to a resolution of $\sim 9''$, and a range of $100 - 307$ Jy beam $^{-1}$ km s $^{-1}$.

Contours: The bright 450 μm emission at a resolution of $\sim 9''$, the contours are: (8, 10, 12, 14, 16, 18, 20, 22, 24, 26, 28, 30) $\times\sigma$, where $\sigma = 50$ mJy beam $^{-1}$.

Table 1
Calibration data

Wavelength	θ_{HPBW}	$S_{\text{tot}}(\text{cal})^{\text{a}}$	$G, \delta G/G^{\text{b}}$	$\sigma_{\text{rms}}^{\text{c}}$	$(f_{20}, f_{60})^{\text{d}}$
850 μm	15.25''	4.56 ± 0.17	265, 15%	10	(1.03, 1.30)
450 μm	8.75''	11.5 ± 1.2	670, 30%	50	(1.45, 2.45)

^a The total flux of CRL 618 in Jy, taken from the JCMT secondary calibrators list, Sandell 1998.

^b The flux gain in Jy/beam Volts⁻¹ and its fractional uncertainty estimated from an extensive set of beam maps and photometry on CRL 618 and Mars.

^c The thermal rms error of the final maps in mJy/beam.

^d The flux correction factor for circular area with $r = 20''$ and $r = 60''$ radius, estimated from beam maps of CRL 618 (see Sandell 1998). If S is the integrated flux density within that area, the error-beam corrected flux is $S_{\text{c}} = S/f$.

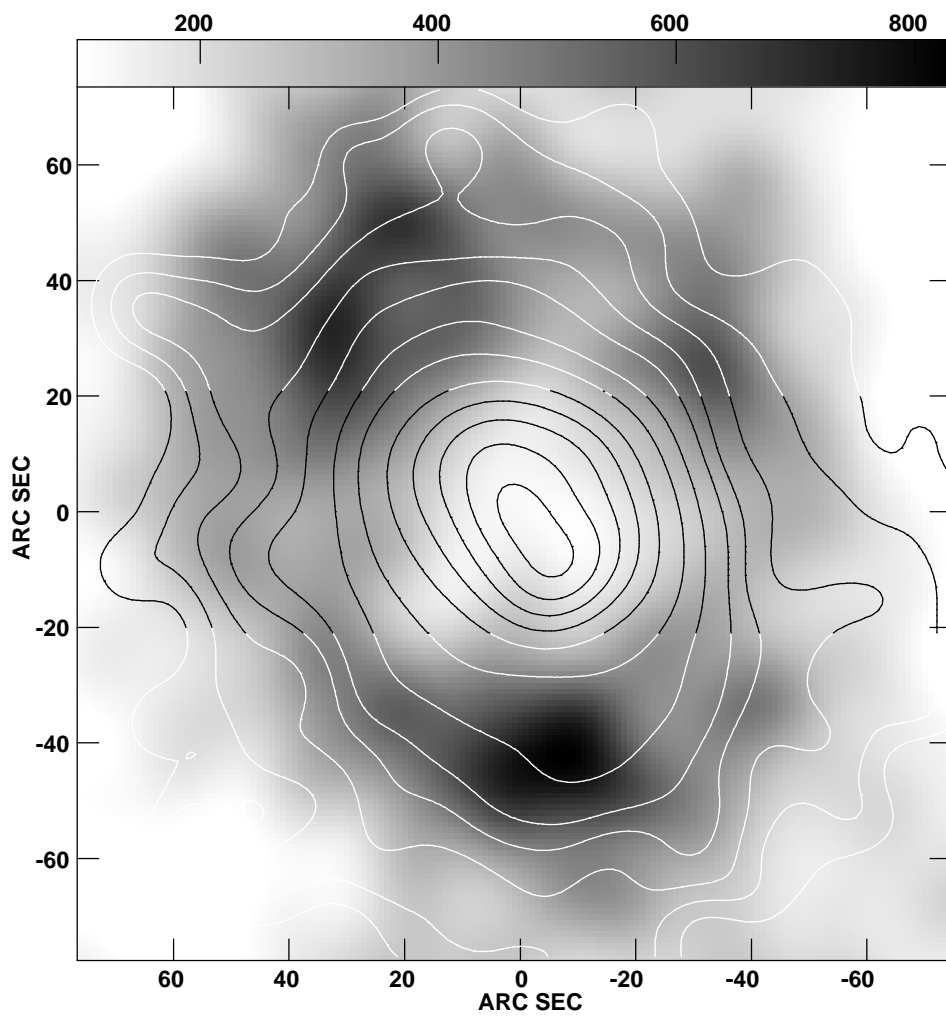
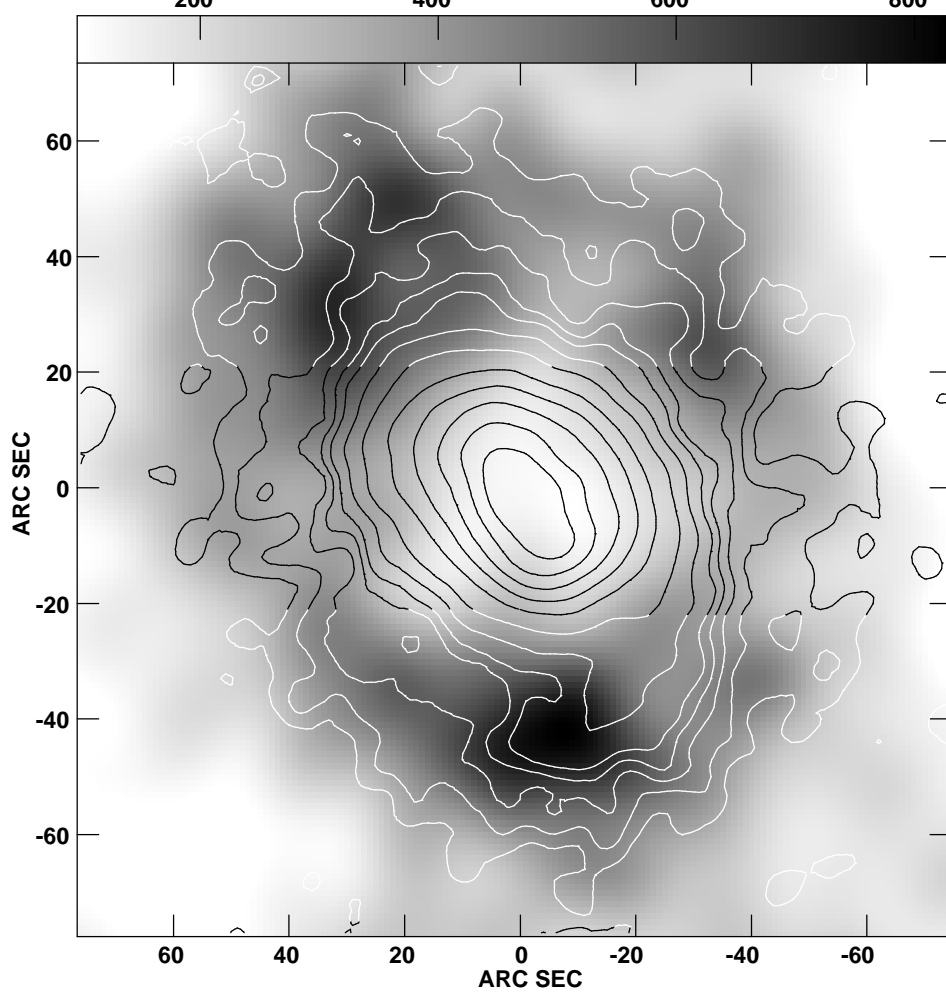


Figure 1

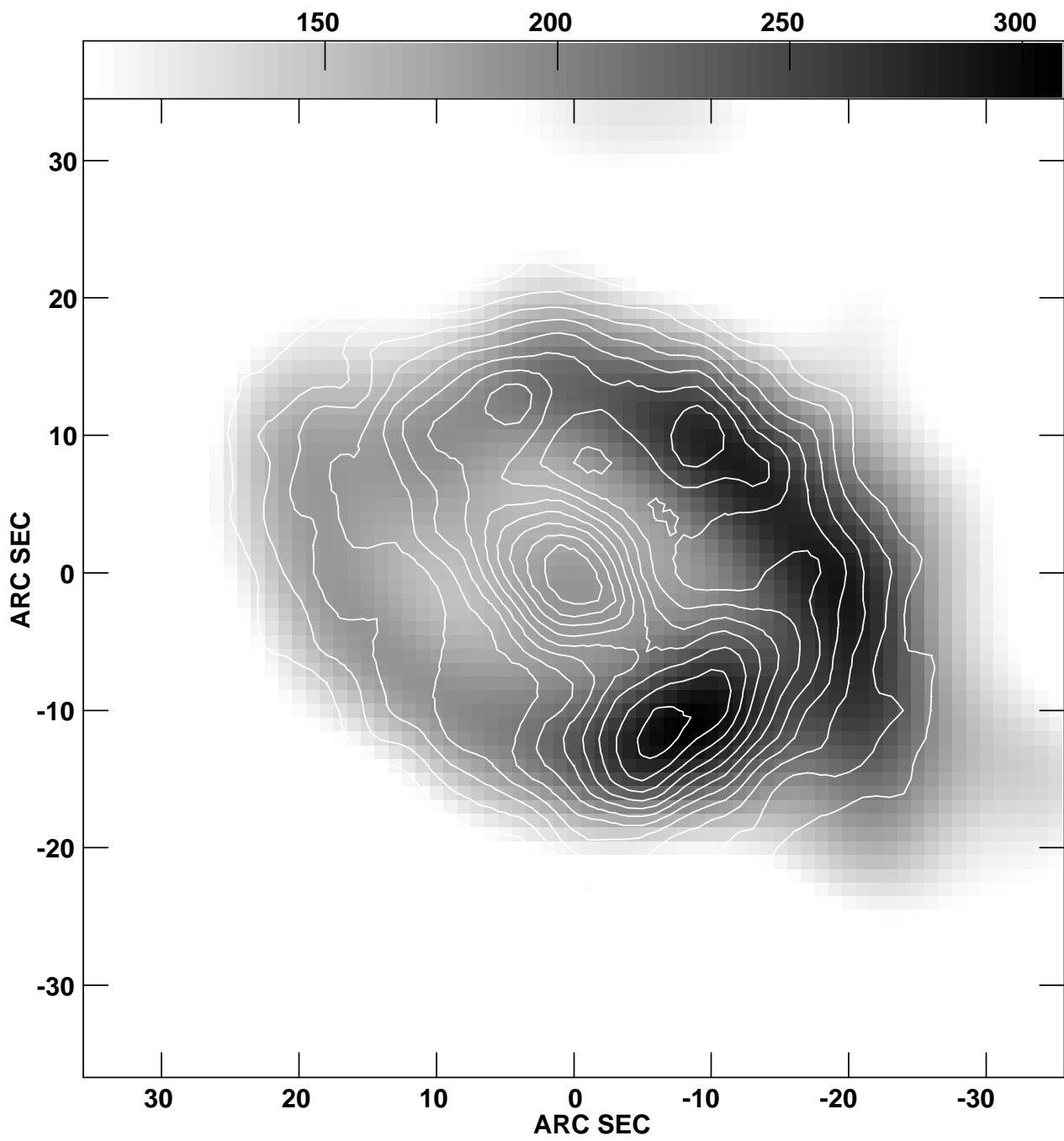


Figure 2